Bifunctional, piperazine-fused cyclic disulfides for oxidoreductase-activated cellular proagents

Lukas Zeisel[1,#], Jan G. Felber[1,#], Karoline C. Scholzen[2], Carina Schmitt[1], Alexander J. Wiegand[1], Leonid Komissarov[3], Elias S.J. Arnér[2,4], Oliver Thorn-Seshold[1,*]

[1] Department of Pharmacy, Ludwig Maximilians University Munich, Butenandtstr. 5-13, 81377 Munich.
[2] Division of Biochemistry, Department of Medical Biochemistry and Biophysics, Karolinska Institutet, SE-171 77 Stockholm, Sweden
[3] Center for Molecular Modeling (CMM), Ghent University, Technologiepark-Zwijnaarde 46, 9052 Ghent, Belgium.
[4] Department of Selenoprotein Research, National Institute of Oncology, 1122 Budapest, Hungary.
[#]The two first authors contributed equally to this work. *Corresponding author.

ABSTRACT: We report piperazine-fused six-membered-cyclic dichalcogenides as rapid-response redox sensors for probes, prodrugs, and bifunctional conjugates that interface with cellular thiol/disulfide redox biology. By combining the thermodynamic stability of 1,2-dithianes with unprecedently rapid kinetics of self-immolation after reduction, these motifs are uniquely reliable and flexible reduction-based sensors for live cell applications. We synthesise four *cis*- and *trans*-piperazine-fused cyclic disulfides and diselenides by scalable, diastereomerically pure, six-step synthetic routes with just one chromatographic purification. Fluorogenic probes using these redox-active diamines are >100-fold faster activated than the previously known monoamines, which now allowed us to deconvolute the kinetics of the reduction and the cyclisation steps during activation. The diastereomers have remarkably different reductant specificity. In particular, the *cis*-fused disulfides are only activated by strong vicinal dithiol reductants, while *trans*-fused disulfides are activated even by monothiols like GSH. Thus, although both disulfides are good substrates for glutaredoxins and thioredoxins in cell-free assays, upon cellular applications the *cis*-disulfide probes substantially report on oxidoreductase activity in the thioredoxin system (the *trans*-disulfides remain promiscuously reactive). Finally, we showcase efficient late-stage synthetic diversification of the piperazine-disulfides, promising their broad applicability as cleavable bifunctional cores for redox probes and prodrugs, for solid phase synthesis, and as linkers for antibody-drug conjugates.

1. INTRODUCTION

Biological research relies on chemical tools with selective reactivity profiles that can be used in living cells. Redox biology remains under-supplied with high-quality chemical tools, particularly in the context of thiol/disulfide redox manifolds: which are used in hundreds of protein networks not only to shuttle electrons but also to modulate protein shape or activity, to control protein-protein interactions, or to trigger or block signaling. The highly conserved, upstream oxidoreductases that supply reducing equivalents for these many reaction manifolds are attractive targets as the "central nodes of thiol/disulfide redox biology": particularly the dithiol-type redoxins, including the thioredoxin/thioredoxin reductase system (Trx/TrxR), the glutaredoxin/glutathione/glutathione reductase system (Grx/GSH/GR), and a handful of related proteins.[1–3]

There are tremendous untapped opportunities for small molecule approaches that are chemocompatible with these dithiol/disulfide chemistries (or even selectively address certain oxidoreductases), and that work effectively and non-invasively in live cells. Such reagents may drive basic research into biological redox dynamics and regulation, support translational medicine with redox- or metabolically-gated diagnostics and therapeutics, or contribute in many other ways to the broader field of chemical biology. A selective reagent platform for the selenol/thiol enzyme TrxR1 was recently developed, relying on the unusual reactivity of its rare active-site selenocysteine.[4] However, there remain no cellularly-effective reagent systems that selectively address dithiol reductases like Trxs and Grxs; and despite some efforts,[5,6] even inhibitors that could be selective for these proteins in the cellular context[7] are not known, regardless of their prominence as cancer-relevant targets[8].

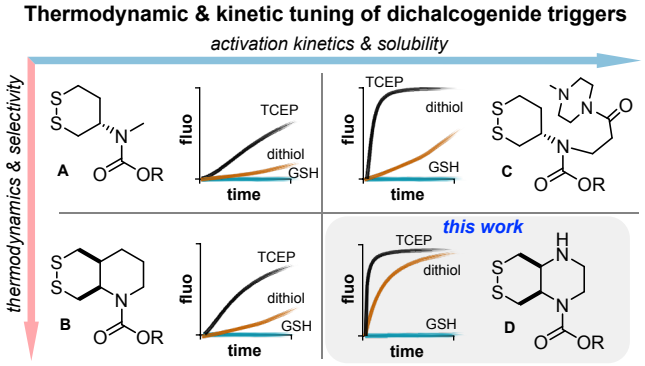

Fig 1 Thermodynamic and kinetic tuning of cyclic dichalcogenide chemistry. We combined the previous designs to establish a condensed molecular core that also enables further derivatisation.

The chemical challenge for targeting these central dithiol reductases is to develop artificial disulfide-type substrates with fast on-target reactivity in cells, yet without broad lability to other (di)thiol proteins or to concentrated monothiols such as GSH. Recently, guided by Whitesides' studies on disulfide thermodynamics,[9] we identified monothiol-resistant cyclic disulfide monoamines **SS60** and **SS66C** as dithiol protein substrates that even offer good selectivity for reduction by Trxs in cell-free assays (**Fig 1A,B**). Their cyclic topology is crucial to dithiol protein selectivity, as it requires full reduction before triggering probe activation;[9] the kinetic and

thermodynamic stabilisation of the 6-membered disulfide were also expected to promote their cellular selectivity by resisting activation from less strongly reducing downstream reductases or GSH. Unfortunately, when these substrates were incorporated into fluorogenic probes, their cargo release kinetics were poor; and they proved to be inactive in cells.[10] This is not surprising since, to be active, their post-reduction dithiol intermediate must cyclise and irreversibly expel a leaving group *before* it is simply re-oxidised by reducing any disulfide in its surroundings: and this dithiol intermediate's similarity to the powerful reductant DTT, that is known to rapidly reduce very many cellular disulfides, suggests that it would need exceptional cyclisation rates to effectively out-compete cellular re-oxidation. We tested using an *N*-methylpiperazinamide (**P**) group to enhance activation kinetics, hoping that local basicity could keep the thiolate deprotonated and so enhance cyclisation. The resulting **P-SS60** (**Fig 1C**) had remarkably faster cell-free activation but still remained cellularly silent.[4] Likely, its post-reduction thiolate cyclisation was still slower than re-oxidation in the cellular environment, or it was too poor a substrate for its target dithiol proteins - or both.

In this work, we wanted to tackle both these potential problems, to develop cellularly-activated proagents triggered by dithiol-type redox effector proteins. We aimed to combine the cyclisation preorganisation delivered by **SS66**-type fused 1,2-dithianes with a nearby amine as in **P-SS60** for local basicity while maintaining the thermodynamic and kinetic disulfide stability that seems to favour their being selective for the powerful Trx/Grx-type dithiol proteins. Condensing these features, we designed *cis*- and *trans*-piperazine-fused cyclic disulfides and diselenides (**Fig 1D**) as a densely-functionalised new class of redox substrate for diverse cellular uses. We aimed to employ them in probes achieving high chemical robustness, fast reduction and cleavage kinetics, and strong dithiol protein selectivity in live cells; we also wanted to explore whether their diamine structure would permit flexible chemical diversification so that they might be broadly applicable well beyond enzyme probes: e.g. as robust but quickly reversible linkers for ADCs or protein purification. Lastly, if the cellular activity were obtained without incurring broad reductant lability, we aimed to test if tuning structural features could enhance processing by selected dithiol proteins as an opening step towards the not only rapid but also highly selective redox probes of the future.

2. RESULTS

2.1 Syntheses of dichalcogenide piperazine redox substrates

Since cargo release, reduction potentials, and reductant sensitivity of annelated dithianes are strongly affected by *cis*- or *trans*-fusion of the bicyclic system; we desired diastereomerically pure synthetic routes that also avoid epimerisation at any of the synthetic steps (from e.g. strong base conditions).[9] We also aimed at scalable synthetic routes that could provide all four disulfide and diselenide piperazines from one starting material type.

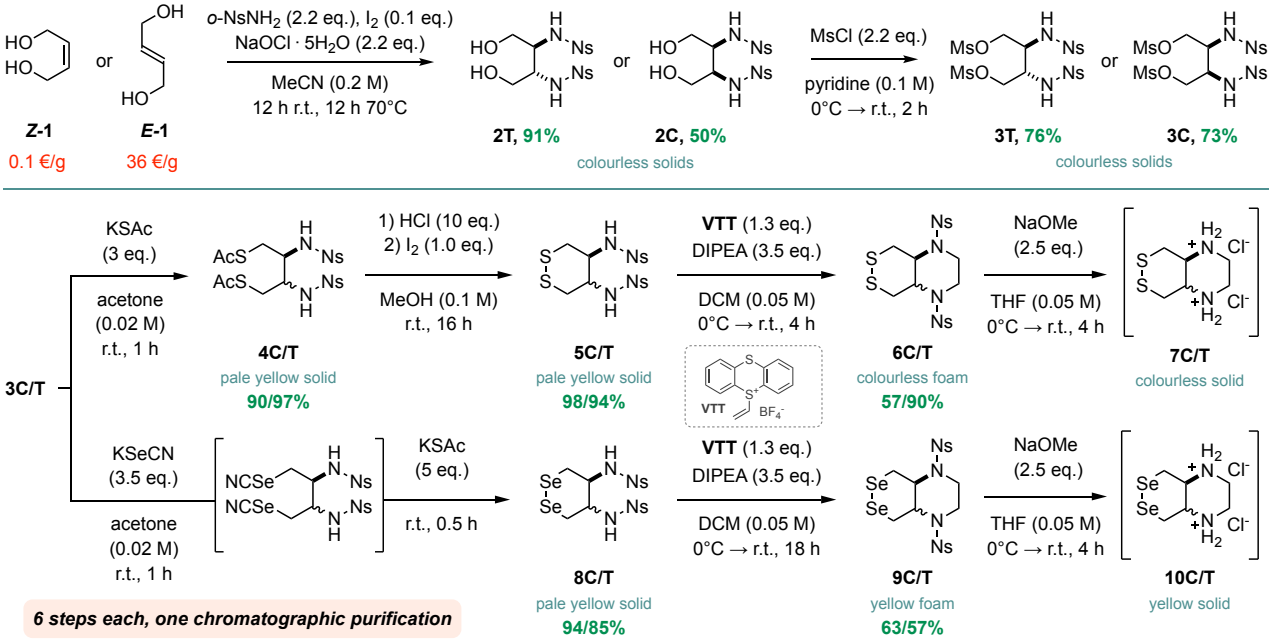

Fig 2 Scalable, modular synthetic procedure for dichalcogenide-fused piperazines.

1,4-dithioerythritol and 1,4-dithiothreitol are alluring starting materials for *cis* and *trans* disulfide piperazines respectively: after oxidation to the dithianes (**DTE^{ox}/DTT^{ox}**), they would only require converting the diol to a piperazine. Unfortunately, DTE^{ox}/DTT^{ox} mesylates and triflates were unsuccessful in C-N bond formation regardless of the *N*-nucleophile used (**DEX/DTX**, **Fig S1**). *Cis*-butene-diol ***Z*-1** is also a cheap feedstock, whose 1,4-diol promises straightforward chalcogen introduction[4,10] but whose alkene may allow alternative 2,3-diamine installations. After 1,4-diol protection, we set up *trans* stereochemistry by epoxidation and basic nucleophilic ring opening, or else *cis* stereochemistry by Upjohn bishydroxylation (**26T/C**, **Fig S1**). We aminated 2,3-diols **26T/C** to the 1,4-dihydroxybutane-2,3-diamines **29T/C** in 4 steps. First, we tested

installing the chalcogens before piperazine formation; in the sulfur series, 1,2-dithiane-4,5-diamines were easily accessed (e.g. **36T/C**), but subsequent reductive amination with glyoxal to assemble the piperazine gave only a complex mixture of species, including the pyrazine formed by oxidation. We then tested forming the piperazine *before* the dichalcogenide: first condensing the open-chain 2,3-diamine with dimethyl oxalate and reducing to the piperazine[11] (e.g. **31**→**39**→**40**, **Fig S1**), then deprotecting the 1,4-diol and introducing the chalcogens, to give bicyclic dithiane target **7T** in 13 steps overall with an overall yield of 6% (**Fig S1**).

Unsatisfied by the high step-count and time-cost of that route, we then tested direct olefin (di-)amination, as pioneered by Sharpless and recently refined by Okumura[12] (**Fig S1**). To our delight, iodine-catalysed 1,2-anti-diamination of starting butenols ***Z*-1** and ***E*-1** provided nosyl-protected 1,4-dihydroxybutane-2,3-diamines **2T/C** as pure diastereomers in good to excellent yield without chromatography (**Fig 2**), cutting 6 steps from the previous route. Diol mesylation gave **3T/C** in excellent purity and good yields by simple precipitation, ready to transform into the 1,2-dithianes and 1,2-diselenanes by using appropriate chalcogen sources (**Fig 2**).

Sulfur was smoothly introduced by treating **3T/C** with KSAc; acidic cleavage of bis(thioester) **4** then oxidation gave protected dithiane-2,3-diamine **5** in near-quantitative yield, again isolated purely by precipitation. (Basic thioester cleavage should be avoided since rapid intramolecular S_NAr onto the nosyl groups gives the aryl thioethers). Now, **5** faced the challenge of annelating the piperazine, which had failed for **36T/C** by e.g. reductive amination. Bis-alkylations of **5** e.g. using 1,2-dihaloethanes did not give good conversion. However, bis-electrophile methodologies from Aggarwal (diphenylsulfonium)[13,14] and Ritter (vinyl thianthrenium "**VTT**")[15] offered alternatives. Diphenylsulfoniums did not perform well with our substrates, but **VTT** gave the piperazines **6T/C** in good yields with purification just over a short silica plug, removing thianthrene as the only reaction byproduct (**Fig 2**). We avoided Fukuyama nosyl deprotection with thiol reagents[16] due to the risk of dithiane reduction then S_NAr; but NaOMe deprotection ran smoothly, and purification by precipitation as the di-hydrochloride gave **7T/C** in excellent yield (63 wt% alongside 2.5 equiv. NaCl, **Fig 2**).

For the selenium introduction, we avoided taking an analogous route to that for sulfur since selenoesters are notoriously unstable[17]. Se could be instead introduced to dimesylates **3T/C** by KSeCN. However, to minimise exposure to selenium species, we aimed to convert the bis-selenocyanates to diselenanes **8** in a one-pot procedure. Again, to avoid intramolecular S_NAr reaction onto the nosyl groups, we did not wish to unmask the selenolates, so avoided *O*-nucleophiles that would perform S_N2 at carbon (RSe**C**N). Instead, we chose KSAc as a chalcophilic nucleophile for deprotection: transiently forming an activated R-SeSAc species that then undergoes intramolecular Se-Se bond formation, presumably via hypervalent selenium. To our delight, the formation of diselenanes **8T/C** was fast and visible by eye (evolution of a bright yellow colour). From here, the procedures matched that for the dithianes, with **VTT** to form the piperazines **9T/C** from the 2,3-nosylamide, then basic solvolytic deprotection, with purification by precipitation, to give piperazine-diselenanes **10T/C**. Interestingly, during the piperazine annelation, both **9C** and **9T** significantly degraded to insoluble solids: presumably ring-opened oligodiselenides, promoted by the strain introduced by the bis(sulfonamide) bicycle; whereas **10T/C** appeared stable.

In summary, we developed a scalable and efficient sequence towards piperazine-annelated 1,2-dithianes (**SS66C**, **SS66T**) and 1,2-diselenanes (**SeSe66C**, **SeSe66T**). The syntheses provide all four dichalcogenides in 6 steps, as pure diastereomers, on a gram scale, and require only one chromatographic purification (**Fig 2**).

2.2 Thermodynamic features of the piperazine-bicycles

We wanted to find out how functional groups near the dichalcogenide affect the thermodynamic stability of the piperazine-annelated systems. In particular, we wanted to compare their performance against that of the corresponding piperidine-annelated systems (**Fig 1B**), to test for influences of their second ring nitrogen: e.g. i) nitrogen lone pair electronics, and bond angle preferences that may distort the annelating ring geometry; ii) the influence of a local basic amine that may lower the local pk_A; or iii) the influence of substituents at the amine that may influence CSSC/CSeSeC-dihedral angles and SS/SeSe bond distance. We determined the reduction potentials of piperazine dithianes **7T/C** by known methods[10], using HPLC to measure reduced-to-oxidised equilibria of model benzamides **H-SS66C-Bz** and **H-SS66T-Bz** against dithiothreitol (DTT; E° -327 mV[18]). Notably, equilibria were reached 10× faster than for piperidine dithianes **SS66C/T-Bz**, although the endpoints were similar: with **H-SS66C-Bz** (−335 mV) harder to reduce than **H-SS66T-Bz** (−317 mV), similar to previous findings[9,10] (**Fig 3a**, **Fig S3**).

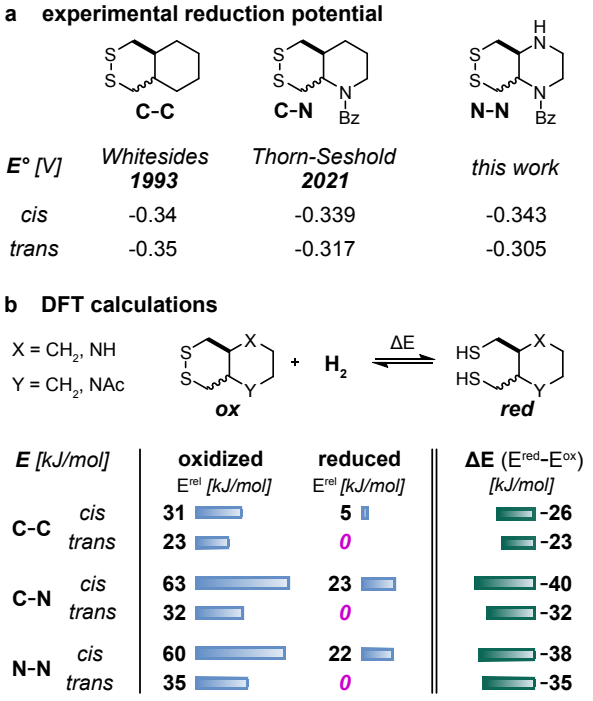

Fig 3 Thermodynamics of bicyclic 1,2-dithianes. (**a**) Experimental reduction potentials[9,10,18] determined by HPLC equilibration against DTT (E° = −0.327 V) (see **Fig S3**). (**b**) DFT calculation of energetic minima - examples for C-C, C-Ac, and H-Ac substitution (see **Fig S4**).

Density functional theory (DFT)-based calculations using the B3LYP functional[19] were performed to look for systematic trends in how annelation influences (i) the relative energies of *cis/trans* diastereoisomers; (ii) ring tension, revealed by SS/SeSe distance and dihedral angles (**Table S2**); and (iii) the energy gain/penalty upon reduction of the dichalcogenides (**Fig 3b**). To that end, energetic minima of oxidized and reduced **SS66C/T** and **SeSe66C/T** species were compared while varying groups in the annelating ring (-CH_2-, -NH-, -NMe-, -NAc-, or -N(CO_2Me)-; see **Table S1**). We were pleased to see that the second, optionally substituted nitrogen atom did not drastically destabilize the bicyclic dichalcogenides. Unsurprisingly, the reduction of **SS66** was much more favourable than that of **SeSe66** (**Fig S4**); but other trends were much smaller, and overall, these calculations did not suggest very different reduction thermodynamics as compared to previous piperidine **SS66** systems (**Tables S1-S2, Fig S4**).

2.3 Redox probes: diversified design and synthesis

To test the kinetic properties of these piperazine dichalcogenides in probes, we incorporated them into fluorogenic probes based on *O*-methylfluorescein (**MF**). As previously established, MF probes are locked as nonconjugated nonfluorescent lactones, so this design allows true off-to-on activation of fluorescence after a reduction-cyclisation-expulsion cascade (**Fig 4a**).[10,20]

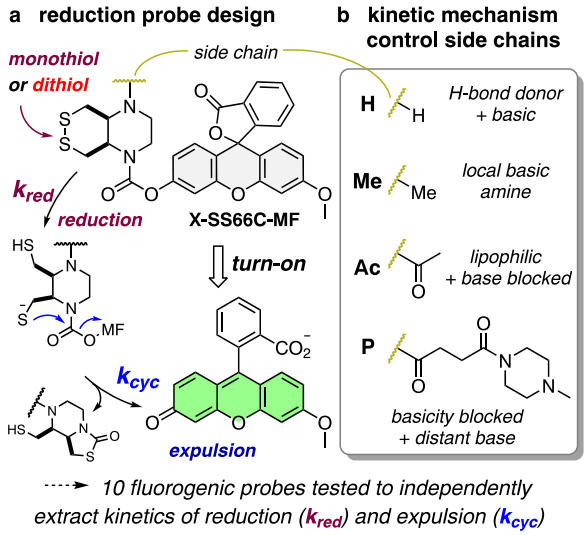

Fig 4 (a) Probes based on carbamates between triggers and 3-*O*-methylfluorescein (**MF**) as a fluorogenic cargo that are activated after reduction (k_{red}) and cargo expulsion (k_{cyc}) steps that re-establish **MF**'s xanthene-based fluorescence.

A major advantage of the piperazines is the potential for diversifying e.g. **H-SS66C/T** probes at the final step of the synthesis, by reactions with the free amine. We now used derivatisations to showcase the modularity of this platform, ultimately preparing a probe library of 16 piperazine dithianes and four additional controls (**Fig S2**). At this stage, we examined the two parent **H-SS66C/T-MF** probes alongside derivatives with three types of sidechain, intended to test the effects of acylation and alkylation on probe performance: methyl (**Me-**, local basic amine, sp^3), acetyl (**Ac-**, abasic, ~sp^2) and succinamidyl-(*N*-methyl)piperazine (**P-**, ~sp^2, distant basic amine) (**Fig 4b**, **Fig S2**). We did not derivatise the **SeSe66-MF** probes, fearing their potential for problematic linearisation as observed during synthesis. All derivatives were accessed in a single step from the free amine precursors in good yields (see Supporting Information). Controls with a non-reducible piperazine-cyclohexane (**H-CC66-MF**) or a **P**-derivatised monocyclic dithiane trigger (**P-SS60-MF**) were also synthesised following similar methods (**Fig S2**).

2.4 Kinetic analysis of reduction-based performance

We aimed to understand the structural influences on the two consecutive kinetic steps involved in the probes' generation of fluorescent signal: (i) reduction (k_{red}); and (ii) cyclisation/cargo expulsion (k_{cyc}) (**Fig 4a**). To separate these steps, we first analysed signal generation kinetics upon reaction with the fast and irreversible reducing agent TCEP (tris(2-carboxyethyl) phosphine): allowing us to extract pseudo-1st-order kinetics of the k_{cyc} step since in our assay conditions, cyclisation and expulsion were rate-limiting (increasing TCEP concentrations did not accelerate fluorescence turn-on; **Fig S5**). We then used this rate to deconvolute reductant-specific k_{red} values from the overall signal generation rates measured with biologically relevant monothiol- and dithiol-reductants GSH and DTT (**Fig S5**).

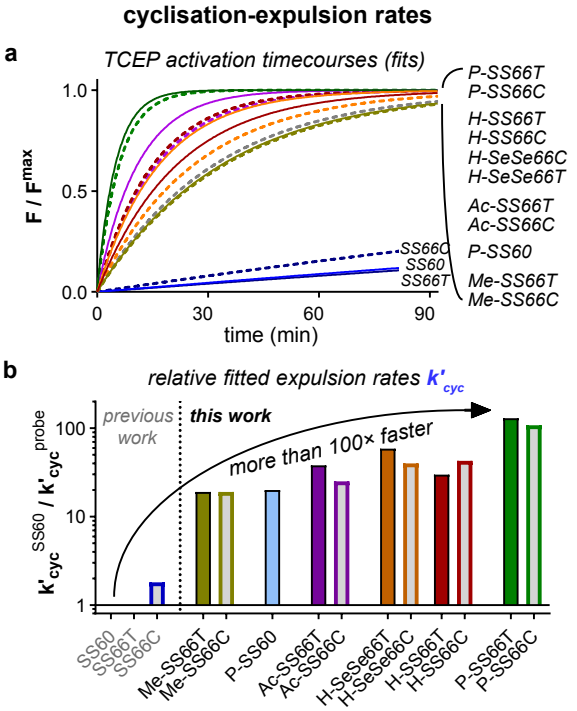

Fig 5 Post-reduction cyclisation kinetics. (**a**) TCEP-mediated activation is fast and irreversible, allowing to fit fluorescence with pseudo-1st-order kinetics reflecting cyclisation/expulsion rates. (**b**) The piperazine-annelated redox triggers give up to >100× faster cyclisation/expulsion kinetics than previous[10] triggers (see **Fig S6**).

The piperazine-fused disulfide probes had vastly faster TCEP-triggered signal generation rates (**Fig 5a**; **Fig S6**) than prior simple dithiane **SS60-MF** and piperidine-dithianes **SS66C/T-MF** (**Fig**

1A,B), which had all had slow activation kinetics that was intrinsically limited by their small k_{cyc} (taking several hours to approach full activation even with a large excess of the quantitative irreversible TCEP)[10]. For the piperazines, even when releasing the electron-rich **MF** phenolate, **P-SS66T/C** showed an exceptional halftime of < 5 min, indicating >100× faster k_{cyc} than **SS66C/T** or **SS60** probes (all with **MF** cargo).

k_{cyc} values for *trans* and *cis* diastereomers of each trigger were closely similar, which is coherent with the assumption that TCEP reduction is both fast and irreversible. However, several trends are apparent when comparing trigger types. The side chain on the piperazines affects k_{cyc}, with **Me** (20×) < **Ac** (30×) < **H** (ca. 50×) < **P** (ca. 110×) (**Fig 5b**; k_{cyc} values are given relative to that for monocyclic **SS60**). Since the bicyclic piperidines **SS66T/C** also had relative rates of just ca. 1-2×, these enhanced rates should *not* be attributed to the triggers' bicyclic structure causing classic Thorpe-Ingold preorganisation. Instead, a large kinetic enhancement can be expected from adding a local basic amine (since **P-SS60** gives ca. 20× enhancement over **SS60**) or from having the second piperazine nitrogen in the ring (e.g. **Ac-SS66T/C** ca. 20× faster than **SS66T/C**), and these effects are somewhat additive (**P-SS66T/C** >100× faster than **SS66C/T**).

We next assayed reduction kinetics with monothiols and dithiols, titrating the cellular monothiol reductant GSH (ca. 5 mM in cytoplasm) and the artificial dithiol reductant DTT (that serves as a cheap model for dithiol proteins) at increasing concentrations and collecting timecourse data (**Fig 6a,b**). DTT gave strong signal generation for all compounds, with 10 mM DTT giving nearly identical signal generation speed as 100 µM TCEP. By contrast, GSH only reduced **SS66T**-type probes: all **SS66C** probes, plus **P-SS60**, **SeSe66T,** and **SeSe66C**, were fully inert to GSH up to 10 mM (**Fig 6c, Fig S7**). Unlike the dithianes, **H-SeSeS66C** was more slowly activated by DTT than *trans*-fused **H-SeSeS66T**.

To compare reduction rates numerically, we considered data where reduction (**Fig S6b**) is orders of magnitude slower than cyclisation; here, the initial signal generation rates (normalised for reductant concentration) approach a maximum $\mathbf{k'_{red}}$ at low reductant concentration, which is a lower bound for the true reduction rate per unit of reductant (**Fig 6c, Fig S8**).

The main feature of interest is that the *cis*-annelated dithianes are remarkably monothiol-resistant, while their *trans*-diastereoisomers are moderately (**Me/H-SS66T**) or even highly (**P-SS66T**) sensitive. We find the *cis*-dithianes' resistance particularly remarkable considering their highly increased cyclisation kinetics compared to previous constructs, which might otherwise have been thought to make them more generally labile. The three last assay types show that the *cis*- and *trans*-diastereomers have very similar thermodynamic reduction potentials (**Fig 3**) and cyclisation rates (**Fig 5**): it is rather their apparent reduction rates $\mathbf{k'_{red}}$ that distinguish them (**Fig 6**). Noting that these $\mathbf{k'_{red}}$ values also reflect the reversibility of the thiol-disulfide exchange (and/or full reduction) steps, one possible explanation for the different monothiol lability/resistance of the **T/C** isomers (a difference that is consistent across so many fluorogenic probes), is that the *trans* diastereomer has a unique kinetic inhibition of retro-reaction after thiol-disulfide exchange (and/or full reduction), potentially by relaxation of a more strained mono/bis-*N*-acylated piperazine ring geometry. Though other factors are also possible, a systematic exploration of the reasons for **T**-instability is best left to future investigations.

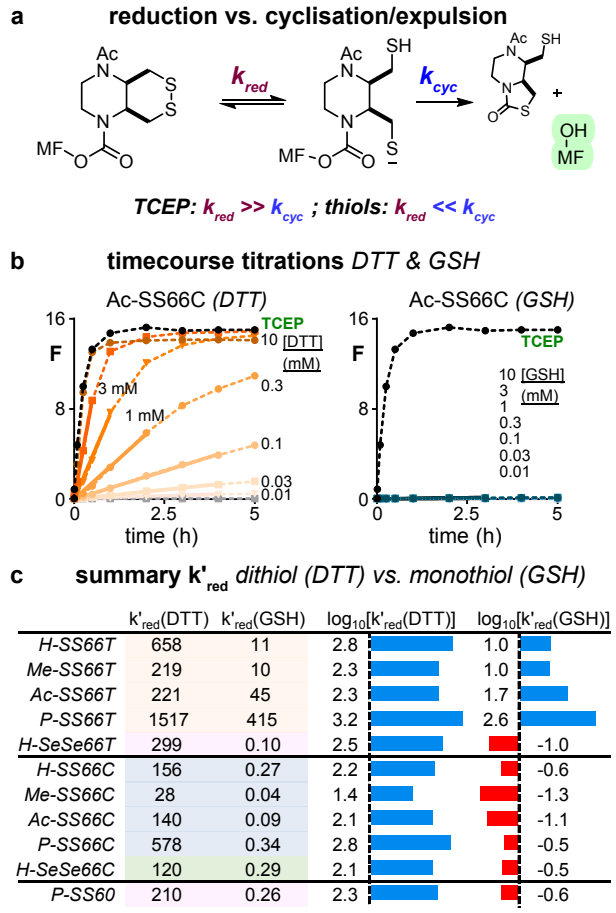

	k'_{red}(DTT)	k'_{red}(GSH)	$\log_{10}[k'_{red}(DTT)]$	$\log_{10}[k'_{red}(GSH)]$
H-SS66T	658	11	2.8	1.0
Me-SS66T	219	10	2.3	1.0
Ac-SS66T	221	45	2.3	1.7
P-SS66T	1517	415	3.2	2.6
H-SeSe66T	299	0.10	2.5	-1.0
H-SS66C	156	0.27	2.2	-0.6
Me-SS66C	28	0.04	1.4	-1.3
Ac-SS66C	140	0.09	2.1	-1.1
P-SS66C	578	0.34	2.8	-0.5
H-SeSe66C	120	0.29	2.1	-0.5
P-SS60	210	0.26	2.3	-0.6

Fig 6 Evaluation of monothiol vs. dithiol reduction kinetics. (a) Simplified mechanism of dithiol- vs monothiol-based **Ac-SS66C-MF** probe activation. (**b**) Dose response timecourses for DTT and GSH (0.01-10 mM) reduction of **Ac-SS66C-MF**. (**c**) Reduction rate constants $\mathbf{k'_{red}}$ for dithiol and monothiol reduction.

2.5 Artifical oxidoreductase substrate character

Building upon the chemical characterisation of fluorogenic disulfide piperazines, we next were interested in assessing their reactivity in biochemical assays with redox-active proteins and enzymes (**Fig 7a**). Generally, and independent of the substitution and diastereomer, disulfide conjugates were activated well within the thioredoxin and glutaredoxin systems and did not notably react with the upstream reductases TrxR1, TrxR2, or GR.

The key observations we had made during chemical characterisation applied nonetheless, with substitution at the idle nitrogen determining release kinetics and (to some degree) enzyme promiscuity along Me<H<Ac<P. Concerning diasteromerism, **SS66T** conjugates' reduction (and thus activation) rates were significantly higher than for **SS66Cs** and thus resulted in faster activation regardless of the enzymatic system used. Adding to the significant background reactivity with GSH as

part of the GR-GSH-Grx system, higher reduction rates of the *trans*-trigger unit appears to render the *trans*-fused probes more promiscuous than their *cis*-counterparts (**Fig S9-S10**): **SS66T** probes were readily activated by glutaredoxins, thioredoxins, and even TRP14. In contrast, **SS66C** probes were unreactive with GSH and TRP14, while being readily activated by Trx1/2 and by Grx1/2, albeit at somewhat different rates.

Diselenanes **SeSe66T** and **C** both reacted with the Trx- and Grx-systems, but to a significantly lesser degree than their sulfur-counterparts – both in terms of slower kinetics and lower absolute fluorescence; though we remain cautious about interpreting the results for diselenane probes (discussion at **Fig S11**).

2.6 Piperazine-dithiane probes are active in live cells

Having determined the *in vitro* selectivity profiles for these piperazine-fused dichalcogen probes, we next turned to cellular assays. At this point, we abandoned diselenane-based probes after initial experiments (**Fig S12**) due to recurring issues with compound degradation and polymerisation: exclusion criteria for meaningful cellular assays.

We were delighted to observe efficient and dose-dependant activation for **SS66T** probes in A549 cells (1-100 µM, **Fig 5b, Fig S12**); activation kinetics and absolute fluorescent signal generation were again determined by the side chain (Me<H<Ac<P). We assessed the role of the thioredoxin system in this signal generation by variation of selenium supply (starvation or supplementation, to decrease or promote synthesis of full-length active seleno-TrxR); by TrxR1 chemical inhibition (using inhibitor TRi-1[21]); or by TrxR1 genetic knockout (from a mouse embryonic fibroblast (MEF) cell line, annotated "fl/fl" for MEF cells expressing TrxR1, "-/-" for the TrxR1 knockout[22,23]). Matching expectations of promiscuity from the cell-free GSH titrations, probe activation was unchanged by all three modulations, showing it was independent of thioredoxin system activity. However, inhibition of GSH-biosynthesis by buthionine-sulfoximine (BSO) reduced activation of **H-SS66T** by almost 50% (**Figures S13-15**). Together with chemical and enzymatic *in vitro* activity assays, this suggests that **SS66T**s function as probes for cellular thiol activity, strongly involving GSH, but at this stage, we cannot exclude roles for redox effector proteins and other protein thiols.

SS66C-based probes were also reliably and dose-dependently activated in A549 cells (**Fig 5c, Fig S12**), but in contrast to their *trans*-counterparts, they provided ca. 10-fold less fluorescent signal. This was not unexpected, as *in vitro* results (**Fig 5a**) indicated monothiol-resistance, thus excluding a major portion of active thiols that likely contribute to the activation of **SS66T**s. To our delight, the three orthogonal methods of modulating thioredoxin system activity all strongly affected **SS66C** activation. Based on earlier *in vitro* assays, we attribute this to modulating the effector protein thioredoxin (**Fig 5c, Fig S14-16**). BSO also causes a notable but smaller effect on **SS66C** activation; since **SS66C** resists direct GSH challenge, we suggest that this effect proceeds through the Grxs that use GSH for recovery. Thus, we propose that all **C**-type probes report on both Trx and Grx activity but are unaffected by cellular monothiols.

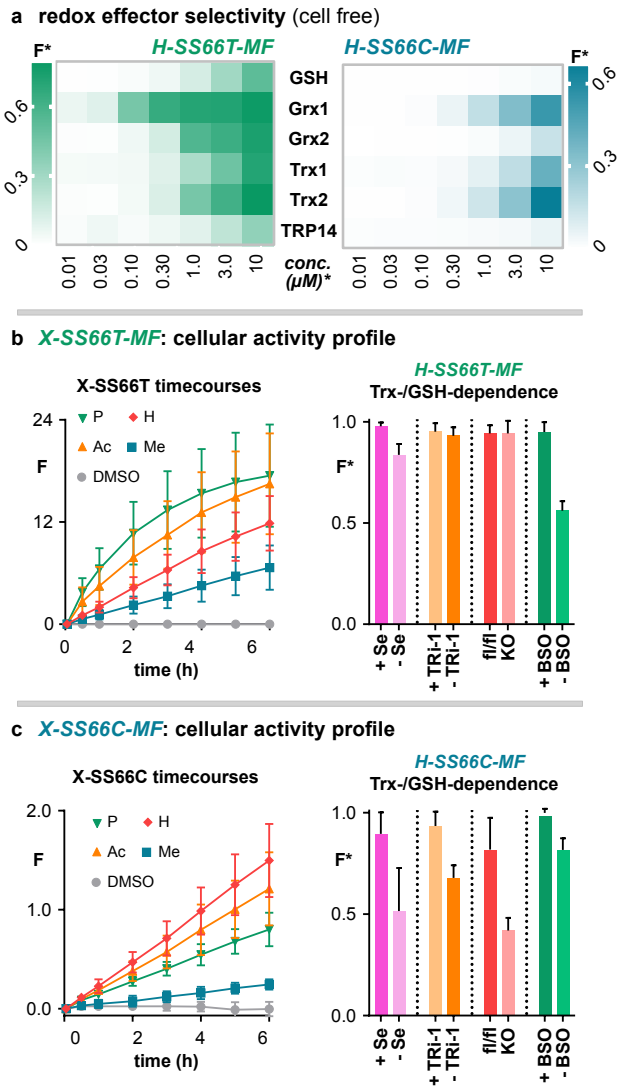

Fig 7 Biochemical and cellular evaluation. (**a**) **SS66C/T** piperpazine probes are artificial substrates for Grx and Trx. Low turnover with TRP14, TrxR or GR. *For GSH, concentrations are given in mM. (**b,c**) Probes based on **SS66T** are strongly activated in A549 cells, whereas **SS66C**s shows 10× lower signal. Dose-dependent linear signal increases over time suggest intracellular turnover. Cellular manipulations of the Trx/TrxR system (±Se, ±TrxR inhibitor TRi-1, TrxR ko vs. wt) gives a significant effect only with **SS66C**-type probes. [F(t) is raw fluorescence intensity; F* is an F(endpoint) value normalised to compare between conditions, defined in cell-free assays as $F^* = [F(3\,h) - F_{blank}(t_0)]/F_{TCEP\text{-}max}$ and in cellular assays as $F^* = [F(6\,h) - F(t_0)]/F_{max}$ where F_{max} is the largest raw F(6 h) replicate value; see Supporting Information Parts 4-5 for details.]

In summary, we identified the first dithiane-based fluorogenic probes that report strongly on cellular redox activity. This advance was enabled by the development of the piperazine-disulfide motif, which provides orders of magnitudes faster probe activation kinetics than literature precedents. We believe that particularly the speed of cyclisation (k_{cyc}) is key for cellular performance, as it determines the efficiency of irreversible fluorophore release and accumulation. Previously known dithiane probes had >100-fold

lower k_{cyc} and thus, even after full reduction by a target species, suffer much more unproductive re-oxidation in a cellular setting. In addition to the mere ability to image cellular thiol-redox activity, we were able to develop probes with orthogonal profiles depending on the diastereomer.

2.7 Dithiane-piperazines as a flexible platform

In principle, we now have developed two orthogonal reduction-activated trigger units: (i) **SS66T** that can be used for the reliable, fast and quantitative release of appended molecular cargos and is activated by thiols of all kinds; (ii) **SS66C** resists reduction by monothiols and is exclusively operated by strong (bio-)chemical reductants like DTT, Trxs and Grxs. Selectivity profiles for both dithiane cores are retained in cellular settings and are independent of sidechain (which rather controls overall activation kinetics). Thus, we envisioned dithiane piperazines as bifunctional motifs which can additionally be equipped with various functionalities to serve many desired applications. To showcase this, we now set out to endow the parent probe **H-SS66C-MF** with a range of useful and broadly applicable functional handles (**Fig 7a**).

We alkylated **H-SS66C-MF** with propargyl bromide (56% yield, **11**) or allyl bromide (90% yield) to provide handles for thiol-ene or thiol-yne chemistry,[24,25] as well as for copper(I)-catalysed azide-alkyne cycloadditions (CuAAC) - the most broadly applied click reactions.[26] Next, we introduced ethylene sulfonyl-fluoride (ESF[27]; 67% yield, **12**), to open up applications to the emerging field of SuFEx chemistry: which is being used from materials chemistry to chemical biology and drug discovery.[28,29] The reductive amination conditions we developed for **Me-SS66C-MF** reproducibly provided aldehyde **13** in good yield (78%) – a compound that offers direct, one-pot functionalisation with amines. To access NHS-esters as a second, orthogonal amine-reactive warhead, we reacted **H-SS66C-MF** with succinic anhydride and TSTU in a two-step protocol (22% yield, **14**). Other reactive groups were introduced by amide couplings: a Fmoc-protected amine (60% yield, **15**) and a cysteine-reactive iodoacetamide (88% yield, **16**).

Overall, we were able to showcase the robustness of the disulfide core under various reaction conditions, including with acid chlorides, strong electrophiles, and under reductive amination. The diverse set of functional handles we introduced onto model probe **H-SS66C-MF** allows for efficient and even high-throughput diversification with orthogonal click(-like) chemistries.

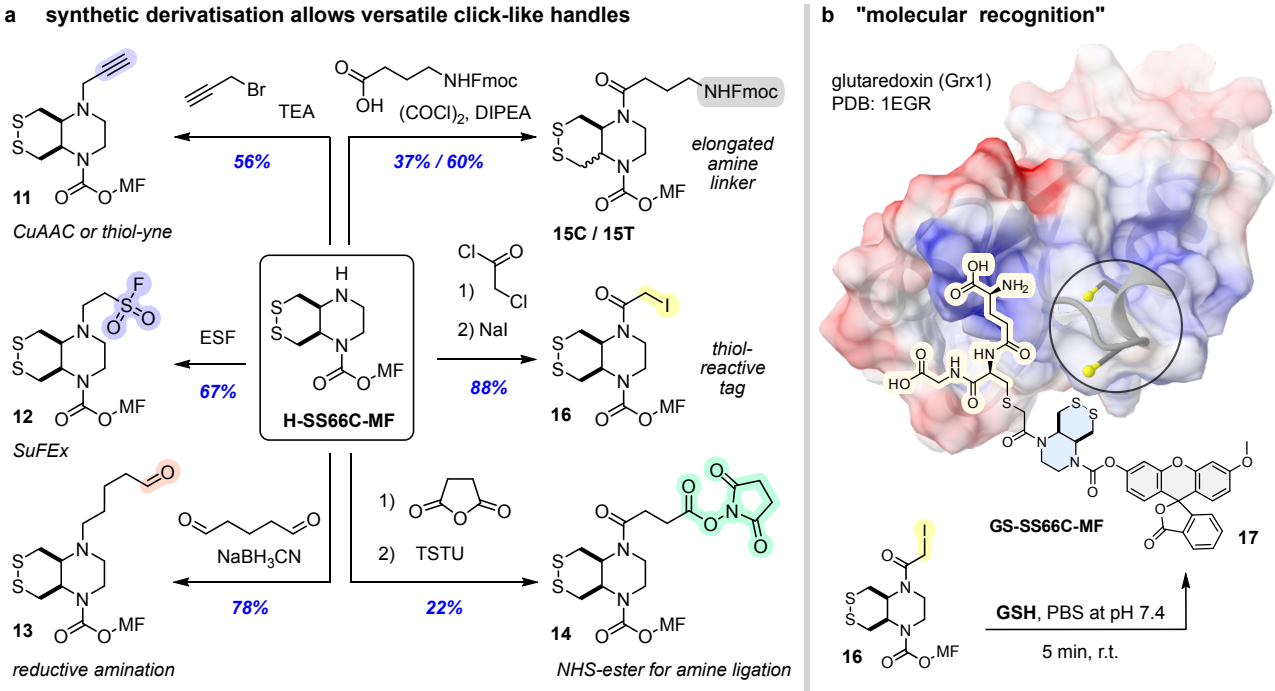

Fig 8 Synthetic accessibility of versatile bifunctional linker based on piperazine-fused 1,2-dithianes. (**a**) Attachment of alkenes or alkynes by alkylation, of sulfonylfluorides by Michael addition, of aldehydes by reductive amination, of elongated amines by amine coupling, of iodoacetamides by and NHS-esters acylation. (**b**) The bifunctional **GS-SS66C-MF** probe as a model compound for chemical Grx recognition.

Finally, to make use of these handles, we aimed to introduce new functionality to our probe. We have already shown that **SS66C**-type probes resist monothiols and can report on cellular Trx/Grx. An outstanding challenge is now to achieve selectivity for one redoxin over the other, despite the structural similarities of Trxs and Grxs and despite their moderate substrate specificities. We imagined that electrostatic complementarity or mismatch between redoxin surfaces and our reporters could add a degree of molecular recognition on top of their dithiol-type chemocompatibility, as a way to address these proteins more selectively.[30] Grx1 distinguishes itself from Trx1 by a defined binding site for GSH,[31] which we envisioned as a suitable chemical recognition motif to enable probe-Grx1 surface complementarity and faster turnover compared to Trx1. We thus alkylated GSH

with iodoacetamide probe **16**, with the reaction in aqueous buffer at pH 7.4, giving full conversion to **GS-SS66C-MF** (**17**) within minutes (**Fig 7b**). In line with the monothiol-stability we established earlier for the SS66C, this establishes another synthetic modality which the dithiane-core is robust to.

We compared model probe **17**'s activation by Trx1 and Grx1 as compared to **H-**, **Ac-** and **P-SS66C-MF**; and identified only a small kinetic Grx1-preference for the **GS-SS66C-MF** probe. Even though this effect was minor, this result is encouraging for the idea of directing redoxin selectivity through introduction of affinity/electrostatic complementarity fragments.

3. SUMMARY AND OUTLOOK

Our previous efforts towards reducible triggers for applications to thiol/disulfide redox biology focused on thermodynamically stable cyclic dichalcogenides that were mechanistically designed to resist monothiol reduction. We had identified *cis*-piperidine-fused 1,2-dithianes as motifs selectively operated by thioredoxins. However, the activation of their fluorogenic probes in cells was poor, which we attributed to slow cyclisation kinetics (k_{cyc}).

In this study, we have improved these cyclisation and cargo expulsion kinetics to achieve workable cellular tools. We assumed that by accelerating cyclisation kinetics, faster turnover would result that could overcome the challenges of cellular release, and that this need not compromise its reductant selectivity profile which would still be predetermined by its topology and geometry. We used disulfide piperazines as a condensed design that combines a cyclic disulfide's redox properties with a basic or derivatisable amine within the bicyclic system to achieve this enhancement: all dichalcogenide piperazine probes were activated at least 20× faster than the previous examples. Building on this assay, we then used titrations with monothiol- (GSH) and dithiol-type (DTT) reductants to extract apparent overall rate constants for the reversible reduction steps ($\mathbf{k'_{red}}$), which had, to the best of our knowledge, not been done for reducible probes so far. The *cis*-fused isomers retained full resistance to reduction by monothiols, while the *trans*-fused isomers were rapidly responsive to both monothiols and dithiols. We also saw that the dichalcogenide piperazines' redox profiles are determined by diastereomerism, and independent of *N*-substitution.

We tested the probes' responses to the GR/GSH/Grx and the TrxR/Trx systems, i.e. the two prominent oxidoreductase systems present in cells. *In vitro*, biochemical assays with isolated proteins showed selective activation of the *cis*-fused series by Trxs and Grxs, but promiscuous reactivity for the *trans*-fused isomers. In cells, and for the first time for any dithiane-based redox probes, we saw dose-dependent activation. The *trans*-fused probe series was activated at high rates and signal intensities; signal generation was independent of modulation of the cellular Trx/TrxR system but responsive to chemical inhibition of GSH biosynthesis. The *cis*-fused probes were activated at lower rates, but this was coherent with their selectivity for dithiol-type proteins, which we validated by the dependence of cellular activation on Trx system activity.

In a conceptual sense, we envision disulfide piperazines as flexibly applicable tools for chemical biology. The modular nature of this system offers the arbitrary choice of a "cargo", e.g. a diagnostic, therapeutic, or other functional agents. For example, similarly to our recent report of thioredoxin-system-targeted bioreductive prodrugs,[32] a **SS66C**-bifunctional linker could be used to gate drug release to redox activity (e.g. releasing duocarmycin-type DNA alkylators[33]). Importantly, the cellular performance, degree of activation, and speed of release will be inherited from one cargo construct to any other since these are defined by the disulfide piperazine chosen. The bifunctionality of disulfide piperazines also offers flexible derivatisation at the second nitrogen for, e.g. tuning probes' physicochemical properties or targeting biolocalisation.[34]

Finally, in a practical sense, to promote the applications of disulfide piperazines, the streamlined 6-step protocol we report that rapidly accesses these piperazines as pure diastereomers on gram-scale will be important; as will the versatile diversification possibilities that they offer e.g. via orthogonal clickable handles. Due to their ease of functionalisation, their stability against non-reductive cleavage, and their remarkably fast reductive cleavage rates, disulfide piperazines may well establish themselves as broadly applicable bifunctional units for redox chemical biology in cells and beyond.

ASSOCIATED CONTENT

Supporting Information

Synthesis, analysis, biochemical evaluations (PDF).

AUTHOR INFORMATION

Corresponding Author

* oliver.thorn-seshold@cup.lmu.de

Author Contributions

L.Z. performed synthesis and analysis, chemoreductant assays, and mechanistic analysis. J.G.F. performed synthesis and analysis, performed chemoreductant, enzymatic specificity screening and DFT-based calculations. L.Z. and J.G.F contributed equally to the design of the experiments, data assembly and visualisation, conceptual analysis of the scientific outcomes, and writing the manuscript, and declare equal shared first authorship. K.C.S. performed biochemical screenings and cellular inhibition and knockout studies. C.S. and A.J.W. performed synthesis and analysis. L.K. performed DFT-based calculations. E.S.J.A. supervised biochemical studies and cell biology. O. T.-S. designed the concept and experiments, coordinated data assembly, and wrote the manuscript with input from all co-authors.

Funding Statement

This research was supported by funds from the German Research Foundation (DFG: SFB 1032 project B09 number 201269156, SFB TRR 152 project P24 number 239283807, SPP 1926 project number 426018126, and Emmy Noether grant 400324123), and the Munich Centre for NanoScience initiative (CeNS) to O.T.-S.; from Karolinska Institutet, the Knut and Alice Wallenberg Foundations (KAW 2015.0063 and KAW 2019.0059), the Swedish Cancer Society (CAN 2018/333 and 19 0330 Pj), the Swedish Research Council (2017-01872), the Hungarian Thematic Excellence Programme (TKP2020-NKA-26), the

Hungarian National Research, Development and Innovation Office (ED_18-1-2019-0025), the Hungarian National Laboratories Excellence program (under the National Tumor Biology Laboratory project, NLP-17), and the Hungarian Ministry of Human Capacities (A´ EEK/41872-16/2020) to E.S.J.A. L.K. has received funding from the European Union's Horizon 2020 research and innovation programme (Grant agreement No 814143).

L.Z. thanks the Fonds der Chemischen Industrie for generous funding through a Kekulé fellowship. J.G.F. thanks the Studienstiftung des deutschen Volkes for support through a PhD scholarship.

ACKNOWLEDGMENTS

We are very grateful to Prof. Tobias Ritter for providing a generous sample of VTT, and the helpful discussions on the reagents' reactivity. We thank Markus Müller for mechanism and kinetics discussion; and Paula Ruppel and Jannick Gehring for synthetic assistance. We also thank Software for Chemistry & Materials B.V. (SCM), Amsterdam for providing us the Amsterdam Modeling Suite (AMS) software for DFT calculations. We thank Marcus Conrad (Helmhotz Centre, Munich) for MEF TrxR1 knockout cell lines.

REFERENCES

(1) Arnér, E. S. J.; Holmgren, A. Physiological Functions of Thioredoxin and Thioredoxin Reductase. Eur. J. Biochem. 2000, 267 (20), 6102–6109. https://doi.org/10.1046/j.1432-1327.2000.01701.x.

(2) Fernandes, A. P.; Holmgren, A. Glutaredoxins: Glutathione-Dependent Redox Enzymes with Functions Far beyond a Simple Thioredoxin Backup System. Antioxid. Redox Signal. 2004, 6 (1), 63–74. https://doi.org/10.1089/152308604771978354.

(3) Jones, D. P.; Sies, H. The Redox Code. Antioxid. Redox Signal. 2015, 23 (9), 734–746. https://doi.org/10.1089/ars.2015.6247.

(4) Zeisel, L.; Felber, J. G.; Scholzen, K. C.; Poczka, L.; Cheff, D.; Maier, M. S.; Cheng, Q.; Shen, M.; Hall, M. D.; Arnér, E. S. J.; Thorn-Seshold, J.; Thorn-Seshold, O. Selective Cellular Probes for Mammalian Thioredoxin Reductase TrxR1: Rational Design of RX1, a Modular 1,2-Thiaselenane Redox Probe. Chem 2022, 8 (5), 1493–1517. https://doi.org/10.1016/j.chempr.2022.03.010.

(5) Powis, G.; Kirkpatrick, D. L.; Angulo, M.; Baker, A. Thioredoxin Redox Control of Cell Growth and Death and the Effects of Inhibitors. Chem. Biol. Interact. 1998, 111–112, 23–34. https://doi.org/10.1016/S0009-2797(97)00148-8.

(6) Baker, A. F.; Dragovich, T.; Tate, W. R.; Ramanathan, R. K.; Roe, D.; Hsu, C.-H.; Kirkpatrick, D. L.; Powis, G. The Antitumor Thioredoxin-1 Inhibitor PX-12 (1-Methylpropyl 2-Imidazolyl Disulfide) Decreases Thioredoxin-1 and VEGF Levels in Cancer Patient Plasma. J. Lab. Clin. Med. 2006, 147 (2), 83–90. https://doi.org/10.1016/j.lab.2005.09.001.

(7) Kirkpatrick, D. L.; Kuperus, M.; Dowdeswell, M.; Potier, N.; Donald, L. J.; Kunkel, M.; Berggren, M.; Angulo, M.; Powis, G. Mechanisms of Inhibition of the Thioredoxin Growth Factor System by Antitumor 2-Imidazolyl Disulfides. Biochem. Pharmacol. 1998, 55 (7), 987–994. https://doi.org/10.1016/S0006-2952(97)00597-2.

(8) Ramanathan, R. K.; Kirkpatrick, D. L.; Belani, C. P.; Friedland, D.; Green, S. B.; Chow, H.-H. S.; Cordova, C. A.; Stratton, S. P.; Sharlow, E. R.; Baker, A.; Dragovich, T. A Phase I Pharmacokinetic and Pharmacodynamic Study of PX-12, a Novel Inhibitor of Thioredoxin-1, in Patients with Advanced Solid Tumors. Clin. Cancer Res. 2007, 13 (7), 2109–2114. https://doi.org/10.1158/1078-0432.CCR-06-2250.

(9) Lees, W. J.; Whitesides, G. M. Equilibrium Constants for Thiol-Disulfide Interchange Reactions: A Coherent, Corrected Set. J. Org. Chem. 1993, 58 (3), 642–647. https://doi.org/10.1021/jo00055a016.

(10) Felber, J. G.; Zeisel, L.; Poczka, L.; Scholzen, K.; Busker, S.; Maier, M. S.; Theisen, U.; Brandstädter, C.; Becker, K.; Arnér, E. S. J.; Thorn-Seshold, J.; Thorn-Seshold, O. Selective, Modular Probes for Thioredoxins Enabled by Rational Tuning of a Unique Disulfide Structure Motif. J. Am. Chem. Soc. 2021, 143 (23), 8791–8803. https://doi.org/10.1021/jacs.1c03234.

(11) Oishi, T.; Hirama, M. Synthesis of Chiral 2,3-Disubstituted 1,4-Diazabicyclo [2.2.2] Octane. New Ligand for the Osmium-Catalyzed Asymmetric Dihydroxylation of Olefins. Tetrahedron Lett. 1992, 33 (5), 639–642. https://doi.org/10.1016/S0040-4039(00)92331-1.

(12) Minakata, S.; Miwa, H.; Yamamoto, K.; Hirayama, A.; Okumura, S. Diastereodivergent Intermolecular 1,2-Diamination of Unactivated Alkenes Enabled by Iodine Catalysis. J. Am. Chem. Soc. 2021, 143 (11), 4112–4118. https://doi.org/10.1021/jacs.1c00228.

(13) Yar, M.; McGarrigle, E. M.; Aggarwal, V. K. An Annulation Reaction for the Synthesis of Morpholines, Thiomorpholines, and Piperazines from β-Heteroatom Amino Compounds and Vinyl Sulfonium Salts. Angew. Chem. Int. Ed. 2008, 47 (20), 3784–3786. https://doi.org/10.1002/anie.200800373.

(14) Yar, M.; McGarrigle, E. M.; Aggarwal, V. K. Bromoethylsulfonium Salt—A More Effective Annulation Agent for the Synthesis of 6- and 7-Membered 1,4-Heterocyclic Compounds. Org. Lett. 2009, 11 (2), 257–260. https://doi.org/10.1021/ol8023727.

(15) Juliá, F.; Yan, J.; Paulus, F.; Ritter, T. Vinyl Thianthrenium Tetrafluoroborate: A Practical and Versatile Vinylating Reagent Made from Ethylene. J. Am. Chem. Soc. 2021, jacs.1c06632. https://doi.org/10.1021/jacs.1c06632.

(16) Kan, T.; Fukuyama, T. Ns Strategies: A Highly Versatile Synthetic Method for Amines. Chem. Commun. 2004, No. 4, 353. https://doi.org/10.1039/b311203a.

(17) Zeisel, L.; Maier, M. S.; Thorn-Seshold, O. Regioselective, Efficient and Scalable Syntheses of 1,2-Thiaselenanes. ChemRxiv 2022. https://doi.org/10.26434/chemrxiv-2022-99slz.

(18) Lukesh, J. C.; Palte, M. J.; Raines, R. T. A Potent, Versatile Disulfide-Reducing Agent from Aspartic Acid. J. Am. Chem. Soc. 2012, 134 (9), 4057–4059. https://doi.org/10.1021/ja211931f.

(19) Stephens, P. J.; Devlin, F. J.; Chabalowski, C. F.; Frisch, M. J. Ab Initio Calculation of Vibrational Absorption and Circular Dichroism Spectra Using Density Functional Force Fields. J. Phys. Chem. 1994, 98 (45), 11623–11627. https://doi.org/10.1021/j100096a001.

(20) Felber, J. G.; Poczka, L.; Scholzen, K. C.; Zeisel, L.; Maier, M. S.; Busker, S.; Theisen, U.; Brandstädter, C.; Becker, K.; Arnér, E. S. J.; Thorn-Seshold, J.; Thorn-Seshold, O. Cyclic 5-Membered Disulfides Are Not Selective Substrates of Thioredoxin Reductase, but Are Opened Nonspecifically. Nat. Commun. 2022, 13 (1), 1754. https://doi.org/10.1038/s41467-022-29136-4.

(21) Stafford, W. C.; Peng, X.; Olofsson, M. H.; Zhang, X.; Luci, D. K.; Lu, L.; Cheng, Q.; Trésaugues, L.; Dexheimer, T. S.; Coussens, N. P.; Augsten, M.; Ahlzén, H.-S. M.; Orwar, O.; Östman, A.; Stone-Elander, S.; Maloney, D. J.; Jadhav, A.; Simeonov, A.; Linder, S.; Arnér, E. S. J. Irreversible Inhibition of Cytosolic Thioredoxin Reductase 1 as a Mechanistic Basis for Anticancer Therapy. Sci. Transl. Med. 2018, 10 (428), eaaf7444. https://doi.org/10.1126/scitranslmed.aaf7444.

(22) Mandal, P. K. Complex Redundancy between the Mammalian Thioredoxin and Glutathione Systems in Cell Proliferation and Tumorigenesis, Ludwig-Maximilian-University Munich, Munich, 2009. https://edoc.ub.uni-muenchen.de/11958/1/Mandal_Pankaj_Kumar.pdf (accessed 2021-08-19).

(23) Mandal, P. K.; Schneider, M.; Kolle, P.; Kuhlencordt, P.; Forster, H.; Beck, H.; Bornkamm, G. W.; Conrad, M. Loss of Thioredoxin Reductase 1 Renders Tumors Highly Susceptible to Pharmacologic Glutathione Deprivation. Cancer Res. 2010, 70 (22), 9505–9514. https://doi.org/10.1158/0008-5472.can-10-1509.

(24) Hoyle, C. E.; Bowman, C. N. Thiol–Ene Click Chemistry. Angew. Chem. Int. Ed. 2010, 49 (9), 1540–1573. https://doi.org/10.1002/anie.200903924.

(25) Hoogenboom, R. Thiol–Yne Chemistry: A Powerful Tool for Creating Highly Functional Materials. Angew. Chem. Int. Ed. 2010, 49 (20), 3415–3417. https://doi.org/10.1002/anie.201000401.

(26) Meldal, M.; Tornøe, C. W. Cu-Catalyzed Azide–Alkyne Cycloaddition. Chem. Rev. 2008, 108 (8), 2952–3015. https://doi.org/10.1021/cr0783479.

(27) Chen, Q.; Mayer, P.; Mayr, H. Ethenesulfonyl Fluoride: The Most Perfect Michael Acceptor Ever Found? Angew. Chem. Int. Ed. 2016, 55 (41), 12664–12667. https://doi.org/10.1002/anie.201601875.

(28) Dong, J.; Krasnova, L.; Finn, M. G.; Sharpless, K. B. Sulfur(VI) Fluoride Exchange (SuFEx): Another Good Reaction for Click Chemistry. Angew. Chem. Int. Ed. 2014, 53 (36), 9430–9448. https://doi.org/10.1002/anie.201309399.

(29) Barrow, A. S.; Smedley, C. J.; Zheng, Q.; Li, S.; Dong, J.; Moses, J. E. The Growing Applications of SuFEx Click Chemistry. Chem. Soc. Rev. 2019, 48 (17), 4731–4758. https://doi.org/10.1039/C8CS00960K.

(30) Berndt, C.; Schwenn, J.-D.; Lillig, C. H. The Specificity of Thioredoxins and Glutaredoxins Is Determined by Electrostatic and Geometric Complementarity. Chem. Sci. 2015, 6 (12), 7049–7058. https://doi.org/10.1039/C5SC01501D.

(31) Begas, P.; Liedgens, L.; Moseler, A.; Meyer, A. J.; Deponte, M. Glutaredoxin Catalysis Requires Two Distinct Glutathione Interaction Sites. Nat. Commun. 2017, 8 (1), 14835. https://doi.org/10.1038/ncomms14835.

(32) Felber, J. G.; Kitowski, A.; Zeisel, L.; Maier, M. S.; Heise, C.; Thorn-Seshold, J.; Thorn-Seshold, O. Cyclic Dichalcogenides Extend the Reach of Bioreductive Prodrugs to Harness the Thioredoxin System: Applications to Seco-Duocarmycins. bioRxiv 2022. https://doi.org/10.1101/2022.11.11.516112.

(33) Felber, J. G.; Thorn-Seshold, O. 40 Years of Duocarmycins: A Graphical Structure/Function Review of Their Chemical Evolution, from SAR to Prodrugs and ADCs. JACS Au 2022, 2 (12), 2636–2644. https://doi.org/10.1021/jacsau.2c00448.

(34) Jia, S.; Lin, E.; Lim, I.; Mobley, E.; Guo, L.; Sletten, E. Water Soluble Chromenylium Dyes for Shortwave Infrared Imaging in Mice. ChemRxiv 2022. https://doi.org/10.26434/chemrxiv-2022-h8rjb.